ASSESSING THE EFFECTS OF CORROSION ON THE MECHANICAL INTEGRITY OF A PIPELINE SUSPENSION BRIDGE

Chris Alexander
Stress Engineering Services, Inc.
Houston, Texas

Henry Cartaya, P.E.
Energistix, Inc.
The Woodlands, Texas

Julian Bedoya
Stress Engineering Services, Inc.
Houston, Texas

ABSTRACT

Work was performed to assess corrosion damage on a pipeline suspension bridge transporting liquid products. Corrosion had been previously detected and characterized using in-line inspection methods. The inspection results were graded and it was noted that several regions had corrosion levels that were of concern. The pipeline company requested that an evaluation be performed on the pipeline bridge that had been constructed during the 1950s.

Evaluation involved construction of a detailed finite element model of the suspension bridge including details on the carrier pipe, an additional support pipe, primary catenary cable, and other supporting cables and wires. The analysis included variations in pipe wall thickness in relation to data collected from the in-line inspection tool run. Loading included gravity, internal pressure, and wind loads. Analysis stress results were then compared to design limit based on the rules of ASME B31.4. The final evaluation revealed that a very specific band of conditions (namely pressure and wind speed) were required to ensure the continued safe operation of the line. Recognizing the need to maintain the required operating pressure, coupled with the inability to control wind speed, led the pipeline company to make repairs to regions of the pipeline where stresses exceeded the code limits. This project was a clear demonstration of how inspection, analysis, and repair methods can work together to ensure the safe operation of pipelines.

INTRODUCTION

This paper provides details on the methods used to assess corrosion in a pipeline bridge. In this study a finite element analysis was done to determine the state of stress for an 8-inch nominal diameter pipe bridge subject to gravity, wind, internal pressure and tension loads from suspender cables used for support. Finite element models incorporating corrosion of the pipeline were modeled using local thin areas (LTA's). This was achieved by defining a thinner section property for selected elements in the model based on actual inspection data provided by in-line inspection efforts. Also, a uniformly corroded pipeline was modeled to determine the minimum required wall thickness that would have adequate structural integrity and be in compliance with ASME B31.4. In addition, removal of suspender cables was simulated until stresses reached unacceptable levels according to B31.4.

MODELING METHODOLOGY

Engineering drawings of the bridge and its components as compiled by the operator were used to construct the finite element models. However, modifications not affecting the results of the study were made in instances where data was incomplete, missing, conflicting or deemed inconsequential. These modifications included not modeling the South and North towers as these structural components of the bridge were considered to be rigid in comparison to the stiffness of the pipeline that was the primary focus of the study.

Consequently, the South and North ends of the catenary cable were fixed at the appropriate locations in space. Similarly, the supports for the wind cables were also fixed at the appropriate location in space. A more detailed description of the boundary conditions is provided in a following section.

The height of the pipeline above the ground was not explicitly noted in the engineering drawings. Therefore, other measurements available in the appropriate engineering drawings were used to scale the dimension in question. The centerline of the 8 inch pipeline was modeled to be 12 feet above the ground level at the towers. Subsequent height measurements relative to a horizontal ground line were made at suspender cable locations. These points were then fit with a polynomial curve to obtain a smooth camber in the pipeline. All dimensions were then examined by comparing photographs of the pipeline bridge were used to ensure that the dimensions used were appropriate.

Finally, an elevation view of the pipeline bridge showed the top of the North tower was six inches higher than the top of the South tower. Conversely, drawings showing the height of the catenary cable and suspender cable dimensions displayed symmetry between the towers. The attachment of the ends of the catenary cable was considered to be at the same height. Figures 1, 2 and 3 show isometric and elevation views, as well as dimensional information used to construct the models.

The finite element model was constructed using the PATRAN modeling package, while analyses and post-processing were performed using the ABAQUS general-purpose finite element code. The pipelines were modeled using standard linearly interpolated 4-noded shell elements with appropriate thicknesses for standard weight nominal 8 inch and 6 inch diameter pipes having wall thicknesses of 0.322 inches and 0.280 inches, respectively. The cables were modeled using linearly interpolated hybrid formulation beam elements. Appropriate circular section properties according to type of cable were assigned in the finite element model. The handline cable spans from South to North tower at a height equal to the smallest suspender cable. The handline cable can be seen in several pictures, but was not included in the finite element model. The omission of this cable does not compromise the results of the finite element model. Additionally, no tension data associated with this component of the bridge assembly was provided in the engineering packet.

Material properties used to model the pipelines and all cables were that of Carbon steel. However, “effective” material properties of wire rope are known to differ significantly from conventional properties for steel. In addition, both the 6 and the 8 inch pipelines were assumed to be filled with water for the purpose of applying a gravitational field. The density used to simulate the weight of the pipes filled with water was 0.3171 lbm/in^3. Elastic modulus and other material and section properties used in the finite element simulations are reported in Table 1.

Boundary Conditions and Loading

The boundary conditions used in the finite element simulations are an idealization of the mechanical response of the actual structure. The out of plane bend in the 8 inch pipeline was idealized as an in-plane radius similar to the way the 6 inch pipeline is constructed and anchored to the ground. This idealization was made given that no corrosion existed in this region of the 8 inch pipeline based on the inspection data and this region does not appear to be a critical region of the structure. Elbow radius information was not available in the engineering drawings that were supplied. A 9 inch radius of curvature was used for the 6 inch pipeline and a 12 inch radius was used for the 8 inch pipeline (i.e. long radius elbows with 1.5R bends). The boundary conditions of the pipelines at the ground were such that all 6 degrees of freedom (DOF) were constrained.

The boundary conditions for the catenary cable at the South and North ends were also constrained in all DOF. The elements in the catenary cable were restricted such that the only rotation allowed was about its main axis. Similarly, the short and long wind cables were restricted in all DOF at what would be the attachment location to the towers. The remainder of the wind cables was restricted in all rotational DOF. Finally, all rotational DOF in the suspender cables were restricted. All cables (except at the anchor points) did not have any translational restrictions.

In order to obtain a stable response from the bridge assembly structure, a sequence of loading events similar to what would be expected during an actual erection of a bridge had to be applied. The loading sequence consisted of first applying a dummy temperature differential to the catenary cable to achieve contraction. Since the cable was anchored in all 6 DOF at the attachment points to the towers, the temperature differential resulted in generating tension in the catenary cable. Since the main objective of this study is to analyze the integrity of the pipeline, the actual tension value in the catenary cable is less important than the tension values in the vertical suspender cables. The second loading step consisted of applying a gravitational field equal to 1G to the pipelines as well as the clamps. Gravity was not applied to the cables given that they represent roughly 10% of the total weight of the entire assembly. The third step involved applying a temperature differential to the suspender cables to approximate the tensions that were reported in inspection data. Once it was verified that all cables were in a state of tension, appropriate internal pressures were applied to the 8 inch and 6 inch pipelines. Finally a wind load corresponding to a 90 mile per hour wind gust, as determined from ASCE 7-02, was applied as a distributed transverse load along the pipelines and clamps. Table 2 summarizes the resulting tension in the suspender cables, and Table 3 summarizes the wind loads applied to the pipeline and clamps. Figures 4 – 7 illustrate the loading sequence in greater detail.

Modeling of Corrosion

Corrosion was modeled by assigning a thinner wall to selected elements in the 8 inch pipeline. Three different corrosion simulations were modeled and include:

1. 50% uniform corrosion – uniform wall thickness in the 8 inch pipeline (i.e., 0.161 inch wall thickness)
2. 75% uniform corrosion – uniform wall thickness in the 8 inch pipeline (i.e., 0.0805 inch wall thickness)
3. Corrosion as reported – spot corrosion as reported in Table 4.

Additionally, a model with no corrosion (i.e., uniform nominal wall thickness in the 8 inch pipeline) was analyzed.

The spot corrosion data presented location inconsistencies with the rest of the data made available to the authors. These inconsistencies included the existence of 26 suspender cables instead of the 21 shown on the engineering drawings. However, it was noticed that corrosion existed in virtually all regions adjacent to the clamps and suspender cables. A total of 48 corrosion patches are reported in the Magpie Systems Inc. report, dated June 20th, 2003; however, assignment of corroded regions according to the report (wheel count, in feet) in the finite element model resulted in regions close to suspender cables N9 and N10 having no corrosion. Therefore, the first corrosion patches implemented were repeated until all adjacent regions to the clamps had corrosion. This resulted in a more conservative estimate of damage to the 8 inch pipeline due to corrosion, and ultimately 53 instances of corrosion instead of the original 48 were modeled. The section properties for the corrosion data are available in Table 4 for ten (10) of the fifty-three (53) sections (representing the most severe and most benign corrosion levels).

MODELING RESULTS

The material used for the modeled pipeline is Grade B with a minimum yield stress of 35,000 psi and an ultimate tensile strength is 60,000 psi per ASME B31.4. Additionally, it is stated in paragraph 402.3.2(d) of ASME B31.4 that “The sum of the longitudinal stress due to pressure, weight and other sustained external loadings shall not

exceed 0.75 S_A". Furthermore, the Code also states "The allowable stress range S_A… for unrestrained lines shall not exceed 72% of the SMYS of the pipe". The allowable bending stress is defined as in Equation (1):

$$\sigma_{Bending,\,a} \le (0.75)\cdot(0.72)\cdot SMYS = (0.75)\cdot(0.72)\cdot 35{,}000psi = 18{,}900psi \quad (1)$$

The allowable hoop stress as set forth in the ASME B31.4 is defined in Equation (2).

$$\sigma_{Hoop,a} = 0.72\cdot\sigma_y = 0.72\cdot 35{,}000psi = 25{,}200psi \quad (2)$$

A total of fifteen (15) different load cases were considered that included variations in boundary conditions, load states, and corrosion levels. The load cases are provided below.

- Case 1: Nominal Wall Thickness, Elastic Constitutive Behavior, Gravity, Tension, Pressure
- Case 2: 50% Uniform Corrosion, Elastic Constitutive Behavior, Gravity, Tension, Pressure
- Case 3: 75% Uniform Corrosion, Elastic Constitutive Behavior, Gravity, Tension, Pressure
- Case 4: Corrosion as reported in Table 2, Elastic Constitutive Behavior, Gravity, Tension, Pressure
- Case 5: Nominal Wall Thickness, Elastic Constitutive Behavior, Gravity, Tension, Pressure, Wind
- Case 6: Corrosion as Reported in Table 2, Elastic Constitutive Behavior, Gravity, Tension, Pressure, Wind
- Case 6A: Corroded Wall, Elastic Constitutive Behavior, Gravity, Tension, Pressure, Wind, Water-filled 8-inch Pipeline, Empty 6-inch Pipeline
- Case 6B: Corroded Wall, Elastic Constitutive Behavior, Gravity, Tension, Pressure, Wind, Reduced Fluid Specific Gravity
- Case 6C: Corroded Wall, Elastic Constitutive Behavior, Gravity, Tension, Pressure, Wind, Reduced Fluid Specific Gravity: Wind Velocity Optimization
- Case 6D: Corroded Wall, Elastic Constitutive Behavior, Gravity, Tension, Pressure, Wind, Reduced Fluid Specific Gravity: Maximum Operating Pressure Optimization
- Case 7: Nominal Wall, Elastic Constitutive Behavior, Gravity, Tension, Pressure, Wind, Less Middle Suspender Cable
- Case 8: Nominal Wall, Elastic Constitutive Behavior, Gravity, Tension, Pressure, Wind, Less Middle Suspender Cable and S4
- Case 9: Nominal Wall, Elastic Constitutive Behavior, Gravity, Tension, Pressure, Wind, Less Middle Suspender Cable, S3 and S4
- Case 10: Nominal Wall, Elastic Constitutive Behavior, Gravity, Tension, Pressure, Wind, Less Middle Suspender Cable, S2, S3, S4, S5, S6
- Case 11: Nominal Wall, Elastic-Plastic Behavior, Tension, Pressure and Gravity ramped to nearly 15g

For brevity detailed discussions will not be provided for each of the load cases. Results for Case 5 are presented and additionally, Cases 6C and 6D were important because they were used by the operator to make decisions about operation of the line and conditions associated with repair. The sections that follow provide details on these particular cases.

Case 5: Nominal Wall Thickness, Elastic Constitutive Behavior, Gravity, Tension, Pressure, Wind

Wind loading generates out of plane deflections due to lateral horizontal forces that are not present in analyses only considering gravity, pressure, and cable tensions. The wind load was calculated based on ASCE 7-02 guidelines on a 90 mile per hour 3 second wind gust. Specific wind load values for the relevant structural components of the bridge are defined in Table 3. Figure 8 shows the out of plane displacements with a scale factor of 1.0 as well as a scale factor of 5.0.

Taking wind loading into account increases the magnitude of all stress quantities reported due to out of plane bending. The Von Mises stress invariant in regions of the tensioned wind cable supports just north of the S8 clamp has a value of 15,995 psi. Figure 9 shows a color plot of Von Mises stresses at this location.

Bending stresses in the same region display a value of approximately 18,179 psi, still under the allowable bending stress of 18,900 psi per ASME B31.4. Figure 10 is the bending stresses contour plots for this particular load case.

Finally, the maximum hoop stress for this case is 13,690 psi (a slight increase from a previous case that did not include wind). Interestingly, the maximum hoop stresses were located just north of the S3 clamp (long South wind clamp) instead of clamp S8 (short South wind clamp).This increase in stress is due to the influence of the out of plane bending caused by the wind load. However, the allowable hoop stress is still less than the allowable hoop stress of 25,200 psi. Figure 11 shows the hoop stress contours in the wind-loaded pipeline.

Uniform Generalized Corrosion Discussion

The results from Case 2 (50% uniform corrosion) suggest that hoop stresses exceed the allowable stresses, and therefore a 50% uniformly corroded wall would likely be inadequate per the ASME B31.4 Code. The bending stress results in Case 1 suggests that if a wind load were to be applied to Case 2 it would also exceed the allowable bending stresses. Case 3 (75% uniform corrosion) exceeds both bending and hoop allowable stress limits by 35% and by 105% respectively, without the application of a wind load. Inclusion of the wind load only exacerbates the already inadequate state of stress in the pipeline.

It is interesting to note that the localized corrosion model, although having corroded regions in excess of 50% (C46), the hoop stresses experienced do not exceed the allowable limit of 25,200 psi as opposed to the generalized 50% corrosion of Case 2. The corrosion-free regions near these “critical regions” in Case 4 provide reinforcement and thus make the state of stress less severe than they would be if they existed without reinforcement in larger sections. However, the corroded regions should be closely monitored and repaired to prevent future corrosion and resulting damage.

Analysis Results for Case 6C

The purpose of the Case 6C was to determine a maximum wind load that would impart stresses not exceeding the allowable bending stress per B31.4. The loads associated with this analysis included tensions as reported in Table 2, gravity, an internal pressure of 975 psi, and various wind loads. Figure 12 shows a plot of wind velocity as a function of maximum stresses in corroded region C46. It is expected that a wind velocity above 44 miles per hour would cause region C46 to exceed the allowable stresses.

Analysis Results for Case 6D

Similar to Case 6C, the purpose of Case 6D was to determine a maximum operating pressure that would not cause stresses that would exceed the allowable bending stress of 18,900 psi. The loads associated with this analysis include gravity, tensions as reported in Table 2, a 90 mph wind velocity, and various internal pressures. Figure 13 shows pressure as a function of maximum stress imparted to region C46.

TECHNICAL LIMITATIONS

Regions where suspender cables have higher tensions are more susceptible to elevated stresses. It is noted that the tension reading results presented in Table 2 deviate in some instances from data included in the inspection report. However, this deviation is not sufficient to warrant significant changes in the conclusions as the results provided herein are conservative. Furthermore, idealizations in the restraint pipeline boundary conditions, as well as the usage of an in-plane radius of curvature rather than the existing pipe bend, raise the stress values near the supports. However, by St. Venant’s principle, stresses far away from these regions are unaffected by these idealizations and thus the conclusions presented are valid.

All analyses performed are quasi-static, and do not consider the energies associated with a suspender cable failing and the sudden application of a load; nor do they consider dynamic effects and corresponding fatigue induced failures.

CONCLUSIONS AND RECOMMENDATIONS

In conclusion, the results suggest that the current corroded state of the pipeline is subject to localized stresses that exceed the allowable bending stress. In addition, it is important to note that whenever multiple corroded regions exist near each other, they reduce the mechanical integrity of the pipeline as they may lack the adequate strength for long term service.

Results from Case 2 suggest that the minimum required thickness for a safe and continued operation of the pipeline bridge relative to hoop stress is in excess of 50% (i.e., a wall thickness greater than 50%). Using the allowable hoop stress per ASME B31.4, a minimum wall thickness of 0.167 inches is calculated – see Equation (3). However, as shown previously, the results of the analyses in Table 5 indicate that the limiting and governing stress in the pipeline bridge is a bending stress.

$$t_{min} = \frac{P \cdot D}{2 \cdot \sigma_{Hoop}} = \frac{975psi \cdot 8.625in}{2 \cdot 0.72 \cdot 35{,}000psi} = 0.167in \qquad (3)$$

Using the maximum bending stress value in Table 5 for Case 5, and solving for the section internal moment due to the combined state of loading a value of 305,993 lb-in is obtained. Refer to equation (4) where M is the section internal bending moment, σ_b is the bending stress as reported in Table 5, and *I* is the second moment of the cross-sectional area of the pipe.

$$M = \frac{\sigma_b \cdot I}{C} = \frac{18{,}179\,lb/in^2 \cdot \left(\frac{\pi}{64}\right) \cdot \left((8.625in)^4 - (7.98in)^4\right)}{4.313in} = 305{,}993lb \cdot in \qquad (4)$$

Using the bending stress equation to solve for the internal diameter with the allowable bending stress substituted, a value of 8.007 inches is obtained for a minimum internal diameter – see Equation (5), where D is the outer diameter of the 8 inch pipe.

$$d_{min} = \sqrt[4]{D^4 - \frac{64 \cdot M \cdot C}{\sigma_b \cdot \pi}} = \sqrt[4]{8.625^4\,in^4 - \frac{64 \cdot 305{,}993lb \cdot in \cdot 4.3125in}{18{,}900\,lb/in^2 \cdot \pi}} = 8.007in \qquad (5)$$

Finally, Equation (6) shows the minimum required thickness with respect to bending.

$$t_{min} = \frac{1}{2} \cdot (D - d_{min}) = \frac{1}{2} \cdot (8.625in - 8.007in) = 0.309\,in \qquad (6)$$

The results in Equation (6) are in agreement with the 96% allowable bending stresses in Cases 5 and 6.

In order to achieve a more uniform state of stress in the pipeline, it is recommended that suspender cables be adjusted to have near uniform tension so that stress concentrations in the pipeline near the clamps and corroded regions are reduced. It is further recommended that all corroded regions be abated with emphasis placed on regions similar to C46. The results of the analyses indicate that the current corrosion conditions are confined to relatively localized regions that do not extend significantly in the longitudinal direction. However, region C46 exceeds the allowable bending stress limit as set forth in B31.4. It is recommended that this region be **repaired**. Corrosion in the other corroded regions approaching the allowable limits should be mitigated. Furthermore, if in the future corrosion develops with greater lengths than analyzed in this report, it was recommended that consideration be made using ASME B31G to designate the need for pressure de-rating or the point at which the corroded pipe will require structural reinforcement.

A final comment concerns the final set analyses of the corroded pipeline (cases 6A-6D) that were performed to determine the maximum permitted combinations of wind and internal pressure. The results indicate that with an internal pressure of 975 psi (MOP), the wind velocity should not exceed 44 mph to ensure that bending stresses remain below the ASME B31.4 limits. Additionally, if the 90 mph design wind load is present, the operating pressure should be limited to 600 psi. Until the pipeline bridge can be repaired using the appropriate repair method, it is recommended that Premcor consider the results provided by the final series of analyses presented in cases 6A – 6D and tabulated in Table 6.

Table 1 - Summary of material and section properties used in finite element model simulations

Component in Bridge Assembly	Elastic Modulus (psi)	Poisson's Ratio	Nominal Diameter (in)	Wall Thickness (in)
Suspender Cables	15,000,000	0.3	0.5	Not Applicable
Handline	Not Modeled	Not Modeled	0.5	Not Applicable
Main Cable (Catenary)	15,000,000[2,3]	0.3	1.875	Not Applicable
Short Wind Cable	15,000,000	0.3	0.625	Not Applicable
Long Wind Cable	15,000,000	0.3	0.875	Not Applicable
8 inch Pipeline (Standard Weight)	30,000,000	0.3	8.0	0.322
6 inch Pipeline (Standard Weight)	30,000,000	0.3	6.0	0.280
8 inch pipeline clamps	30,000,000	0.3	9.875	0.625
6 inch pipeline clamps	30,000,000	0.3	7.875	0.625
Vertical portion of clamps	30,000,000	0.3	Not Applicable	1.25

NOTES:
1. Density of steel (0.281 lbm/in^3) added to density of water (0.0361 lbm/in^3)
2. Wire Rope User's Manual, Third Edition, 1993
3. Properties of a 6x19 IWRC wire rope.

Table 2 - Comparison of tension readings for Finite Element Method (FEM) results, and prior inspections

Suspender Cable Number	FEM Tensions (lbs)	Year 1999 Tensions	Year 2003 Tensions
S10	1,721	2,455	1,625
S9	1,979	1,545	900
S8	1,567	1,460	800
S7	882	1,345	750
S6	265	1,385	850
S5	846	1,310	700
S4	2,519	1,345	900
S3	500	Cable too short	1,056
S2	1,580	Cable too short	Cable too short
S1	719	Cable too short	Cable too short
MIDDLE CABLE	1,975	Cable too short	Cable too short
N1	716	Cable too short	Cable too short
N2	1,577	Cable too short	1,056
N3	490	Cable too short	850
N4	2,486	1,425	1,056
N5	863	1,270	700
N6	264	1,345	750
N7	882	1,345	750
N8	1,567	1,460	1,111
N9	1,980	1,545	750
N10	1,731	1,425	Missing data

Table 3 - Summary of wind load resultants on structural components

Structural Component	Wind Load (lb)
8 inch pipe	6,400
6 inch pipe	4,900
Vertical part of clamp	191

Table 4 - Spot corrosion data as reported by in-line inspection

Corrosion Group	% Metal Loss	Resulting Wall Thickness (in)
C1	22	0.251
C29	22	0.251
C41	43	0.184
C42	45	0.177
C46	51	0.158
C48	21	0.254
C50	27	0.235
C51	76	0.077
C52	27	0.235
C53	63	0.119

Table 5 - Critical stress results for pipeline suspension bridge under various loading conditions

Stress Measure (psi)	**Case Number and Description**									
	Case 1: Nominal Wall Thickness, Elastic Constitutive Behavior, Gravity, Tension, Pressure	Case 2: **50%** Uniform Corrosion, Elastic Constitutive Behavior, Gravity, Tension, Pressure	Case 3: **75%** Uniform Corrosion, Elastic Constitutive Behavior, Gravity, Tension, Pressure	Case 4: Corrosion as reported in Table 4, Elastic Constitutive Behavior, Gravity, Tension, Pressure	Case 5 [1,2,3]: Nominal Wall Thickness, Elastic Constitutive Behavior, Gravity, Tension, Pressure, Wind	Case 6 [2,3,5]: Corrosion as reported in Table 4, Elastic Constitutive Behavior, Gravity, Tension, Pressure, Wind	Case 7: Nominal Wall, Elastic Constitutive Behavior, Gravity, Tension, Pressure, Wind, Less MID Suspender Cable	Case 8: Nominal Wall, Elastic Constitutive Behavior, Gravity, Tension, Pressure, Wind, Less Suspender Cables (MID,S4)	Case 9: Nominal Wall, Elastic Constitutive Behavior, Gravity, Tension, Pressure, Wind, Less Suspender Cables (MID, S3,S4)	Case 10: Nominal Wall, Elastic Constitutive Behavior, Gravity, Tension, Pressure, Wind, Less Suspender Cables (MID, S2,S3,S4,S5,S6)
Von Mises Stress[4]	11,539	22,839	44,879	20,015	15,995	24,267[5]	16,158	16,063	16,335	24,847
Bending Stress	10,835	17,454	**25,645**	14,603	18,179	**26,589[5]**	18,565	18,680[5]	18,779	**24,467**
Hoop Stress	13,002	**26,137**	**51,838**	23,008	13,364	23,039[5]	13,870	13,829[6]	13,779	17,698
Allowable Bending Stress	**18,900**									
Allowable Hoop Stress	**25,200**									

NOTES:

1. Stress values adjacent to short South wind cable clamp. Refer to **Figures 27**, **28** and **29**
2. A less conservative simulation yielded the following results: Von Mises stress=13,465 psi; Bending stress=14,670 psi; Hoop stress=13,355 psi.
3. The wind load was made less conservative by changing the coefficient of drag from 1.2 (conservative) to 0.9 (as outlined in Figure 6-21 in SEI/ASCE 7-02, pg.71.
4. Von Mises stress is calculated as

$$\sigma_{VM} = \left[\frac{(\sigma_1 - \sigma_2)^2 + (\sigma_2 - \sigma_3)^2 + (\sigma_3 - \sigma_1)^2}{2} \right]^{1/2}$$

where σ_1, σ_2 and σ_3 represent principal stresses calculated from the component stresses.

5. A less conservative simulation using a coefficient of drag of 0.9 versus 1.2 yielded the following results: Von Mises = 22,176 psi; Bending = **23,290** psi; Hoop = 23,029 psi
6. Stress values marked in **BOLD** exceed the respective allowable bending or hoop stress per ASME B31.4.

Table 6 - Summary of results for corrosion cases with modified loading conditions

Stress Measure (psi)	**Case Number and Description**				
	Case 6: Corroded Wall Elastic Constitutive Behavior, Gravity (water filled 6" and 8" pipeline), Tension, Pressure, Wind – Region C46	Case 6A: Corroded Wall, Elastic Constitutive Behavior, Gravity (empty 6" pipeline, water filled 8" pipeline), Tension, Pressure, Wind – Region C46	Case 6B: Corroded Wall, Elastic Constitutive Behavior, Gravity (empty 6"pipeline, specific gravity of 88% for fluid filled 8" pipeline), Tension, Pressure, Wind – Region C46	Case 6C: Corroded Wall, Elastic Constitutive Behavior, Gravity (empty 6"pipeline, specific gravity of 88% for fluid filled 8" pipeline), Tension, Pressure, Wind Optimization – Region C46	Case 6D: Corroded Wall, Elastic Constitutive Behavior, Gravity (empty 6", specific gravity of 88% for fluid filled 8" pipeline), Tension, 90 mph Wind, Pressure Optimization – Region C46
Von Mises Stress[4]	24,267	17,546	17,541	17,546	17,541
Bending Stress	**26,589**	**23,521**	**23,488**	**23,521**	**23,488**
Hoop Stress	23,039	21,417	21,429	21,417	21,429
Allowable Bending Stress	**18,900**				
Allowable Hoop Stress	**25,200**				

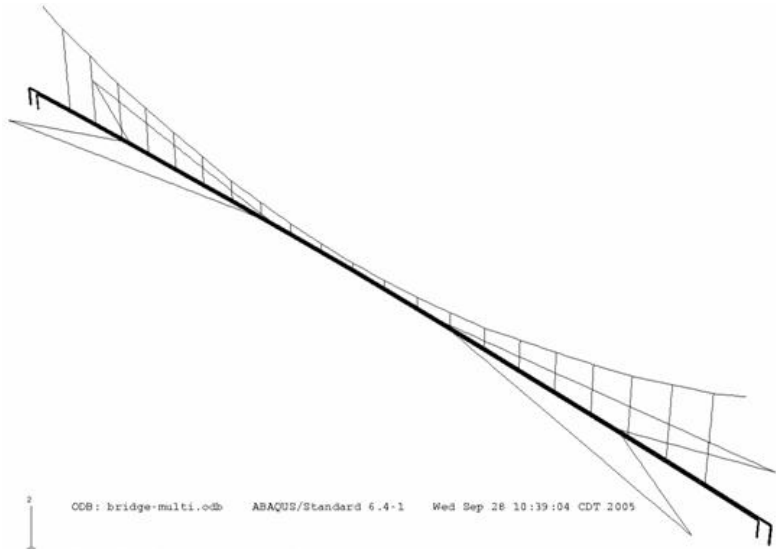

Figure 1 - Isometric view of finite element model of Cal Sag Crossing Pipeline Bridge

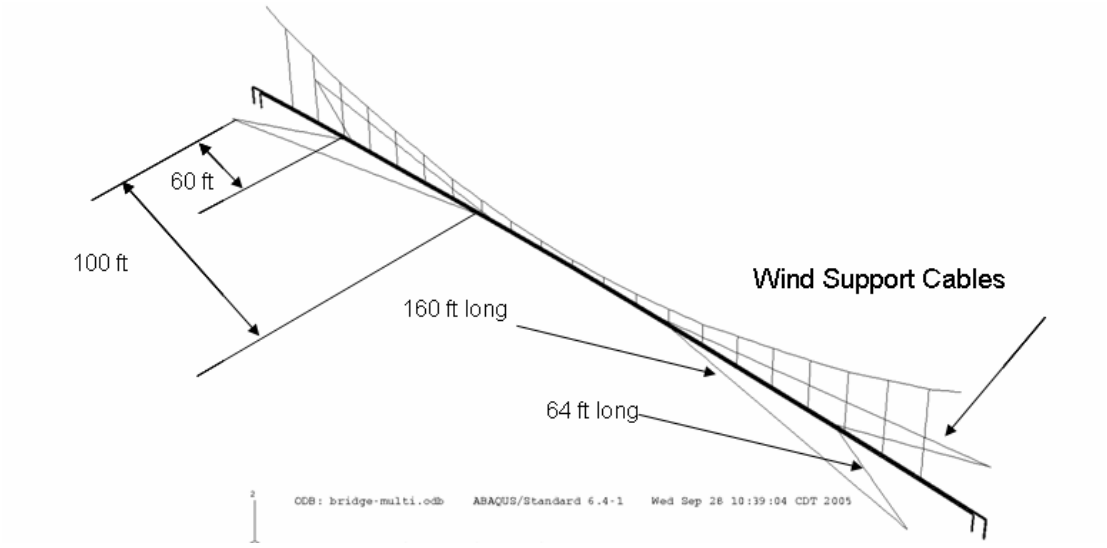

Figure 2 - Wind support cable dimensions and relative location

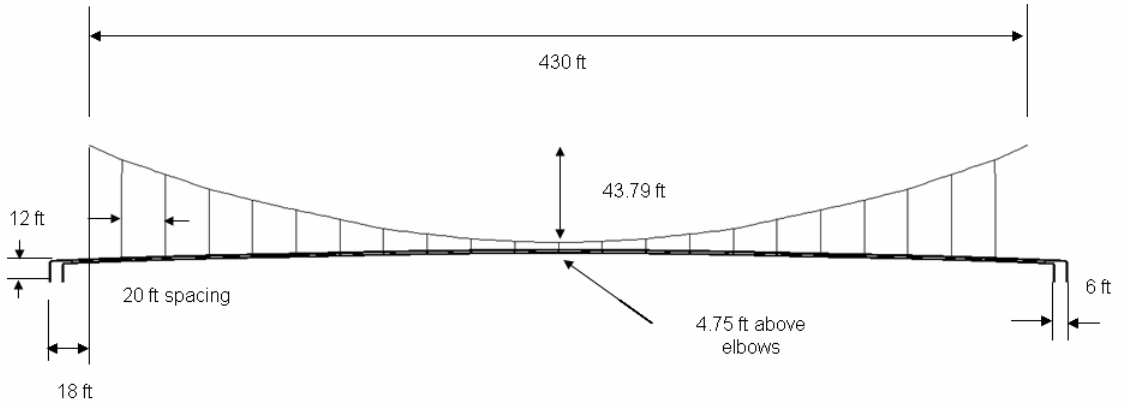

Figure 3 - Overall dimensions used in finite element simulations

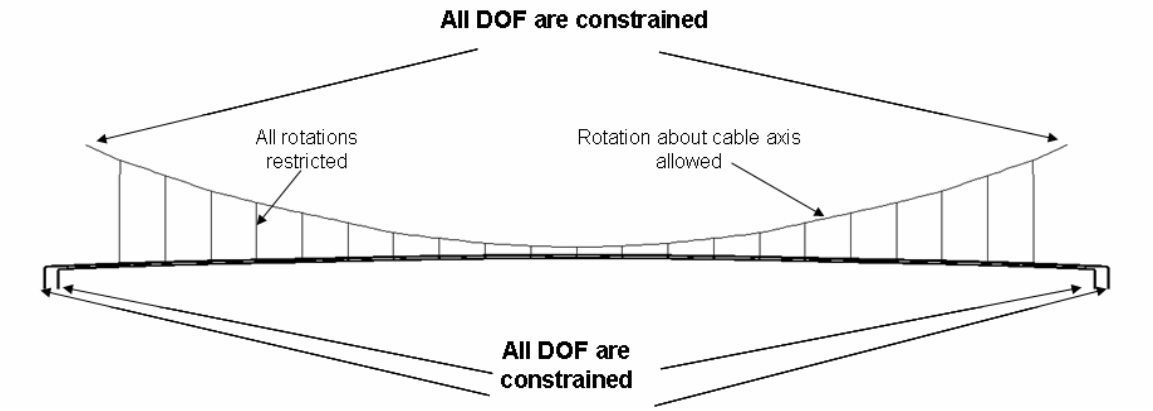

Figure 4 - Boundary conditions applied to pipelines, suspender cables, and catenary cable
(similar boundary conditions to short and long wind cables are also applied (not shown))

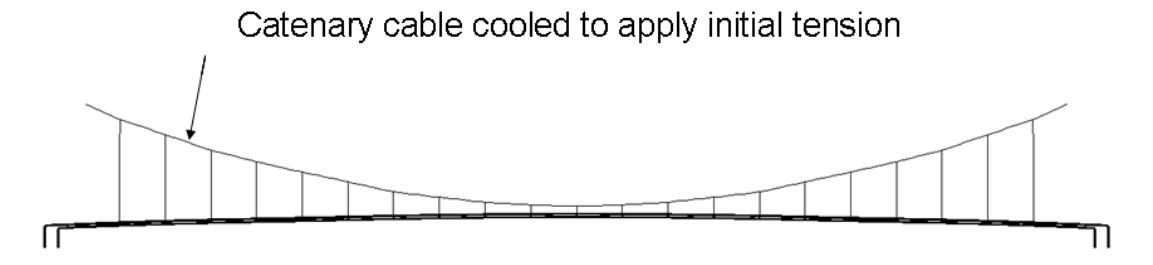

Figure 5 - First step in loading sequence
(temperature differential applied to the catenary cable to induce an initial tension)

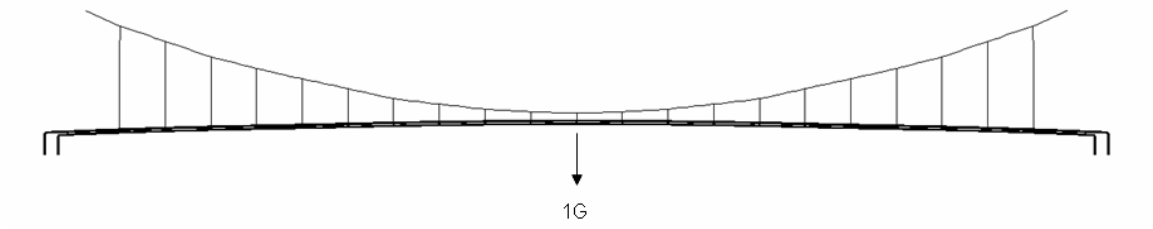

Figure 6 - Second step in loading sequence
(gravitational field equal to 1G to pipeline and clamps)

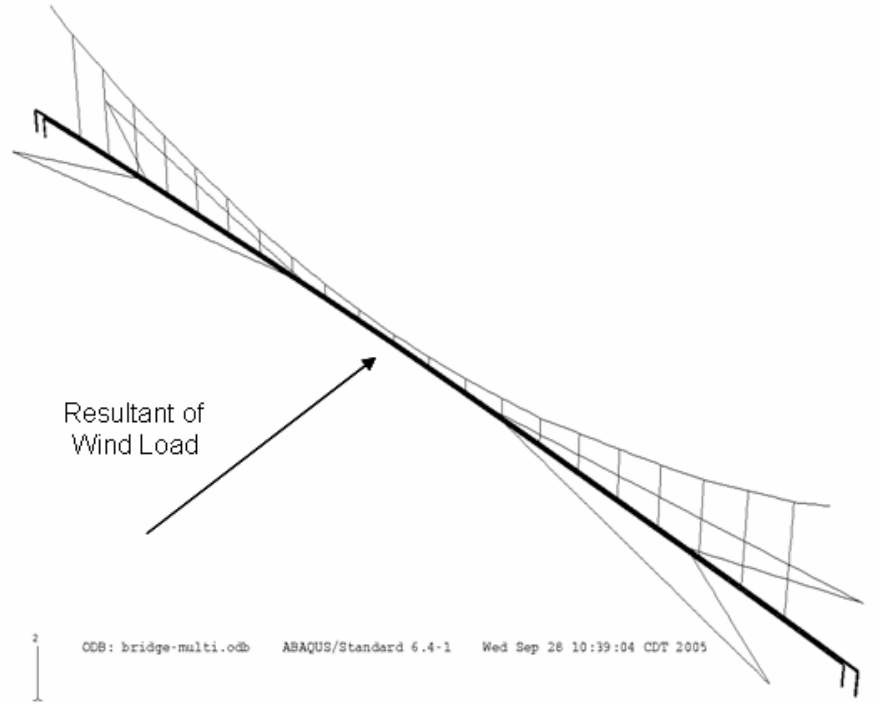

Figure 7 - Resultant of wind load applied to pipelines and clamps

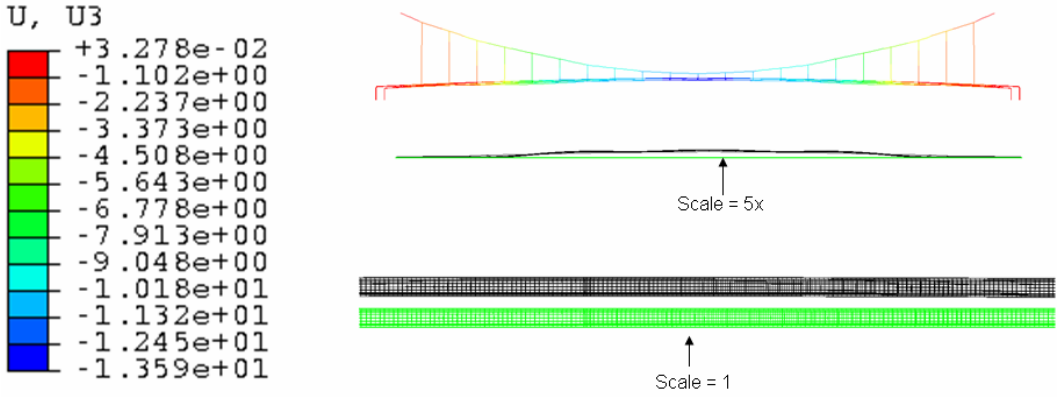

Figure 8 - Out of plane displacement for uniform wall thickness with a transverse wind load applied. Color scale applies to first two plots from top to bottom. The remaining plot represents the original (green) and deformed (black) geometries

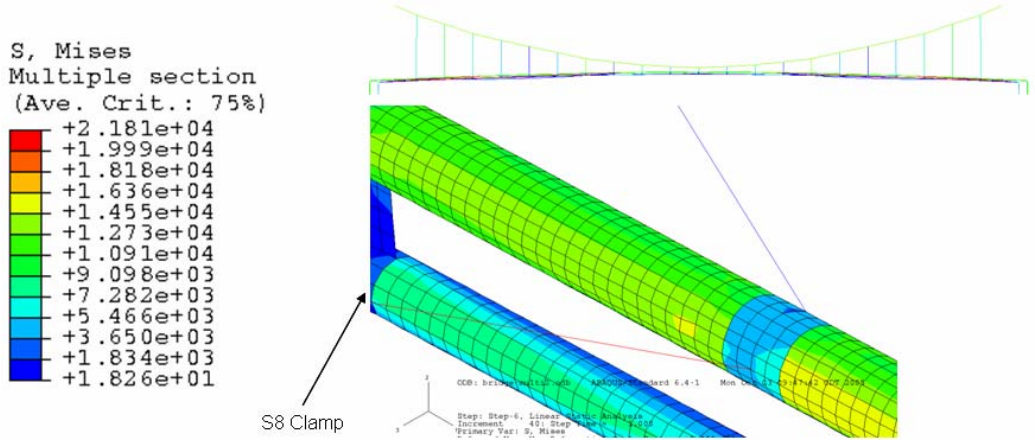

Figure 9 - Von Mises stress distribution with gravity, internal pressure, tension and wind

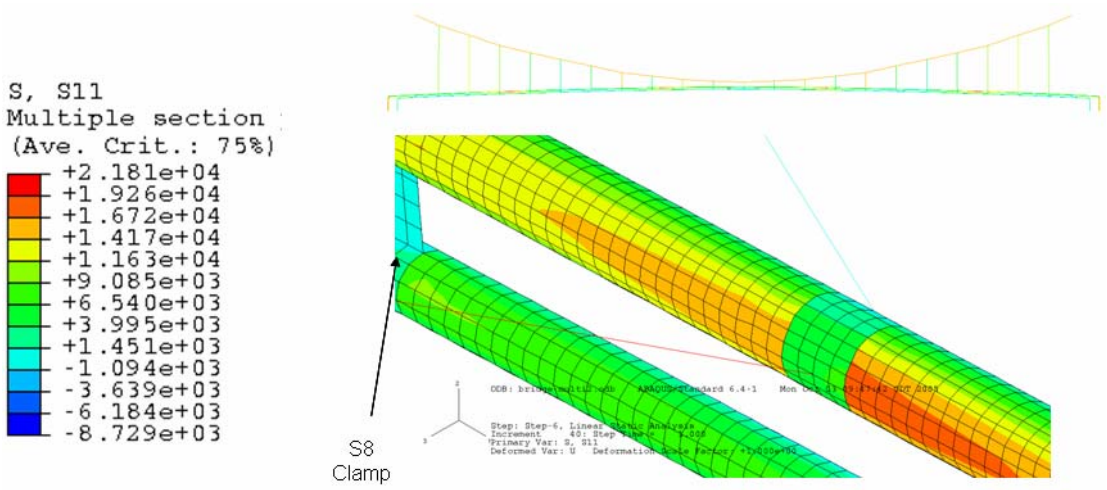

Figure 10 - Bending stresses for pipeline under gravity, tension, internal pressure and wind loads

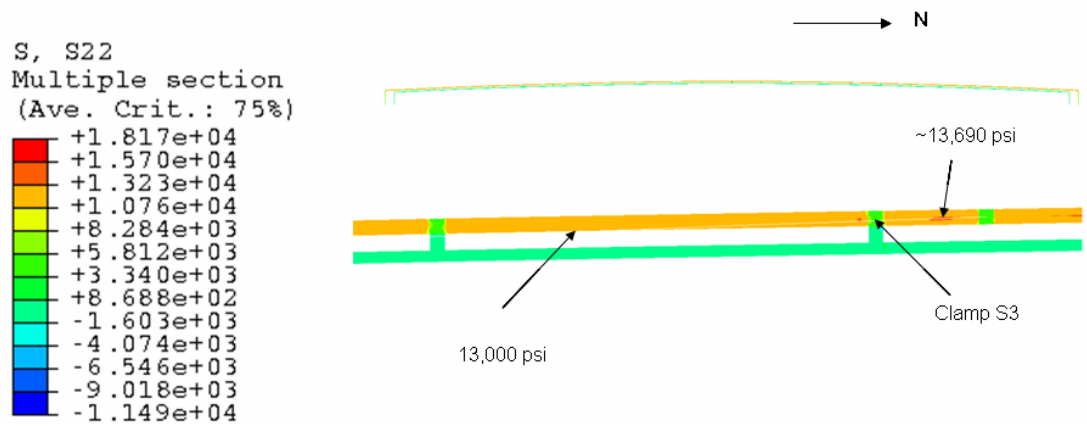

Figure 11 - Hoop stress distribution at several locations for the pipeline subject to gravity, tension, internal pressure and wind. Note the location of the highest stresses is different from that of bending

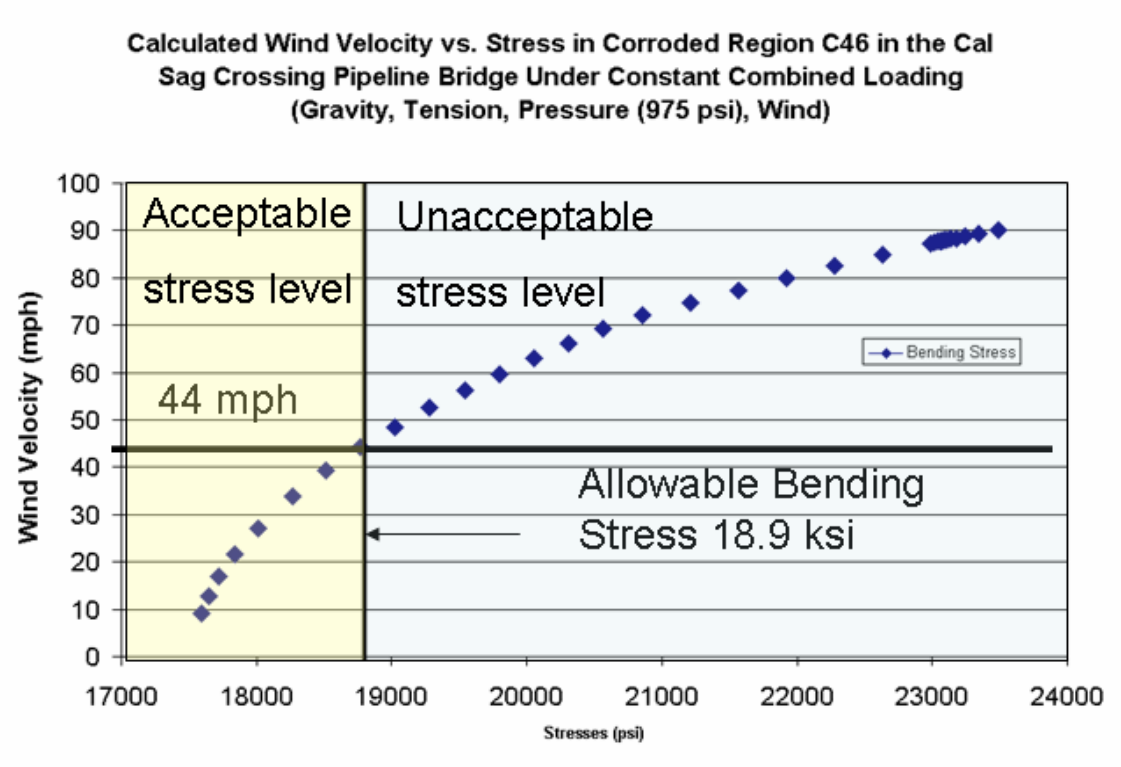

Figure 12 - Wind velocity as a function of imparted stresses to corroded region C46

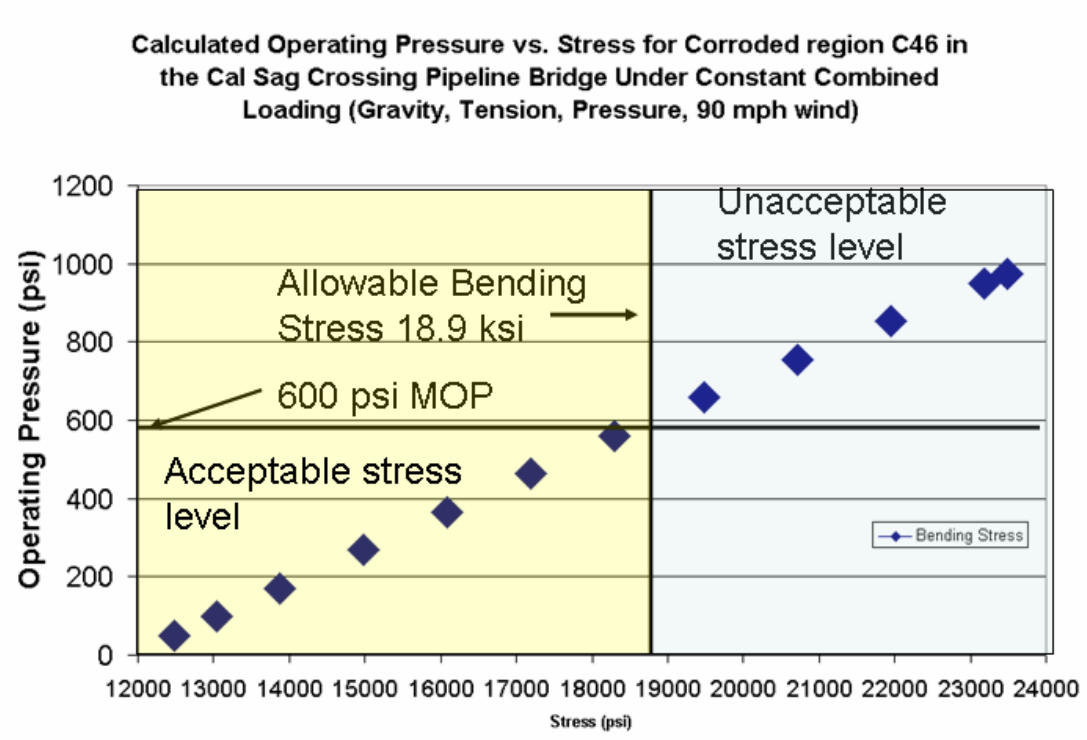

Figure 13 - Pressure as a function of bending stress for corroded region C46